ACS APPLIED MATERIALS & INTERFACES

Research Article

www.acsami.org

# 4-Dimethylaminopyridine Promoted Interfacial Polymerization between Hyperbranched Polyesteramide and Trimesoyl Chloride for Preparing Ultralow-Pressure Reverse Osmosis Composite Membrane

Jiaxu Qin,[†] Saisai Lin,[†] Shuqin Song,[‡] Lin Zhang,*[,†] and Huanlin Chen[†]

[†]Engineering Research Center of Membrane and Water Treatment Technology of MOE, Department of Chemical and Biological Engineering, Zhejiang University, Hangzhou 310027, China

[‡]State Key Laboratory of Optoelectronic Materials and Technologies, School of Physics and Engineering, Sun Yat-sen University, Guangzhou 510275, China

Supporting Information

**ABSTRACT:** We have presented a concept of ultralow-pressure reverse osmosis membrane based on hyperbranched polyesteramide through interfacial reaction promoted by pyridine derivate. In this strategy, a key catalyst of 4-dimethylaminopyridine, which can both eliminate the steric hindrance of acyl transfer reaction and facilitate the phase transfer in interfacial polymerization, is adopted to drive the formation of a thin film composite membrane from the hyperbranched polyesteramide and trimesoyl chloride. The results of the characterization demonstrate that a dense, rough, and hydrophilic active layer with a thickness of about 100 nm is formed when the 4-dimethylaminopyridine catalyst is used. The salt rejections for $Na_2SO_4$, NaCl, and $MgSO_4$ of the as-prepared composite membrane are higher than 92%, especially for $Na_2SO_4$ with 98% rejection. The water fluxes reach about 30−40 $L{\cdot}m^{-2}{\cdot}h^{-1}$ even at an operation pressure of 0.6 MPa. The membrane exhibits good chlorine-resistance ability but poor resistance abilities to acidic and alkaline solutions in the physical−chemical stability experiment. It is also found that the resultant membrane possesses excellent separation performance for PEG-200, showing a promising way to separate small organic molecules from water.

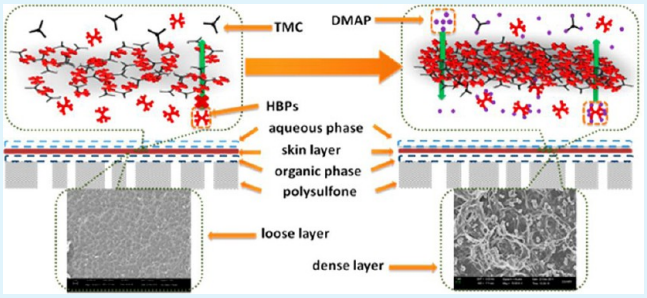


**KEYWORDS:** *hyperbranched polyesteramide, multifunctional catalyst, reverse osmosis membrane, ultralow-pressure*

## 1. INTRODUCTION

Desalination is considered as an effective method of producing freshwater and alleviating the pressure on water resources. Over 15 000 desalination plants have been installed in the world to date, and global water production through desalination is predicted to exceed 38 billion $m^3$ per year in 2016.[1] More than 50% of these desalination plants are reverse osmosis (RO) plants, which is attributed to the application of robust membranes.[2] Such widespread application leaves no doubt that even a small improvement on the water permeability of RO membranes would significantly reduce the total energy and economic cost. Therefore, the development of RO membranes with excellent permeation flux and reasonable rejection has become a main trend in RO desalination.

Currently, commercially available RO membranes are mainly derived from aromatic polyamides (PA) through interfacial polymerization (IP) between diamine and acyl chloride monomers.[3,4] These thin film composite (TFC) membranes exhibit satisfactory separation properties because the fact that the quite thin and relatively hydrophilic composite layers due to the existence of self-inhibition of IP and numerous hydrophilic amide groups, respectively, endow TFC membranes with relatively high water flux, and the rigid benzene framework ensures excellent salt/organic rejection simultaneously.[5−7] While the compact stack structure of the composite layer can produce a remarkable permeation resistance as well, leading to the generally high operation pressure and energy consumption of PA RO membranes.

The improvement of membrane performance in this circumstance is particularly important and has been researched using different methods such as the addition of nanoparticles and organic additives,[8−15] the change of reactive monomers,[16,17] and the modification of RO membrane surface, which includes grafting or coating new materials.[18−24] However, these methods can improve the water flux or decrease the operation pressure at the expense of other performances such as rejection.

However, if we can develop the skin layer into a thinner but defect-free three-dimensional network instead of the traditional compact stack one based on some new types of functional

Received: April 12, 2013
Accepted: June 24, 2013
Published: June 24, 2013

  

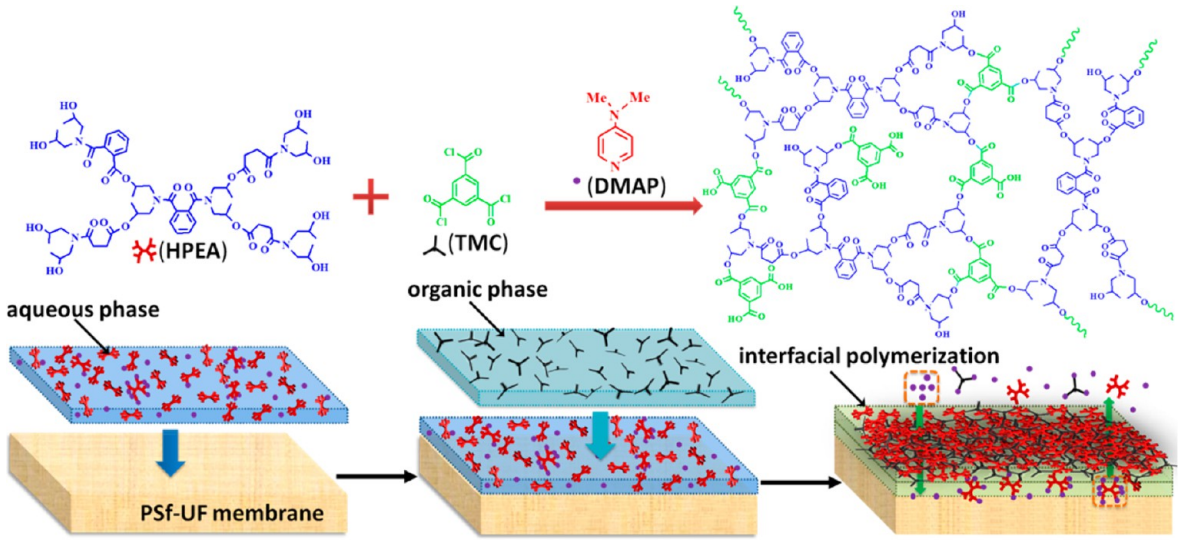


**Figure 1.** Schematic illustration of the interfacial polymerization in the preparation process of the PSf-HPEA + DMAP composite membrane.

monomers, the permeation resistance of RO membrane can be much lower without a sacrifice of the rejection, making it possible to possess high water flux and high salt rejection for the RO membrane simultaneously. And the hyperbranched polymers (HBPs) are just such a kind of macromolecule that are highly branched and possess numerous reactive terminal groups, expected to form this three-dimensional network structure possibly.[25−30] HBPs have usually been used as additive, precursor, and cross-linking agent in the preparation of membranes.[31−35] It has been reported that hyperbranched polyethyleneimine (PEI) and hyperbranched polyamidoamine (PAMAM) were used to prepare TFC membranes by IP with trimesoyl chloride (TMC) as cross-linking agent.[36,37] However, these membranes are just defined as nanofiltration (NF) membranes with a low corresponding rejection for univalent salt.[38] In the above case, since the diffusion of HBPs into the other phase and their polymerization are more difficult than the traditional diamine aqueous monomer because of the large steric hindrance, which also lowers the reactivity of HBPs, the as-prepared membranes are consequently very loose with defective skin layer. And in our previous work, by reducing the steric hindrance effect of PEI, we succeeded in improving the separation performance of the composite membrane significantly, prepared with PEI and TMC through IP.[39] Therefore, the improvement of the reactivity of HBPs with TMC is the key to realizing the application of HBPs in RO membranes preparation.

As known, 4-dimethylaminopyridine (DMAP) is an effective catalyst for acyl transfer.[40,41] When acylating sterically hindered secondary or tertiary alcohols with carboxylic anhydrides or acyl halides, its catalytic activity is approximately $10^4$ times higher than that of pyridine.[42] Moreover, it has been estimated that DMAP is also a kind of R4NX-type phase transfer catalyst (PTC).[43] Therefore, we chose DMAP as the catalyst to promote IP between HBPs and TMC. Considering the fact that the rigid benzene rings of PA promise traditional RO membrane an excellent rejection for salts, hyperbranched polyesteramide (HPEA), which is a typical aromatic secondary alcohol with a high steric hindrance, was adopted as the aqueous monomer (Supporting Information Figure S1b). Our attempt opens the possibility of preparing ultralow-pressure RO membranes based on hyperbranched polymers.

## 2. EXPERIMENTAL SECTION

**2.1. Materials.** All the reagents and chemicals were of analytical grade and were used just as received. The polysulfone ultrafiltration (PSf-UF) supporting membrane, with a molecular weight cutoff of 30 000, was provided by the Development Center for Water Treatment Technology, Hangzhou, China. Hyperbranched polyesteramide (HPEA, M.W. = 1200) was purchased from DSM (Netherlands). The other reagents and chemicals were purchased from Sigma-Aldrich Chemicals, including trimesoyl chloride (TMC), 4-dimethylaminopyridine (DMAP), and salts.

**2.2. Fabrication of HPEA-Based Composite Membranes.** The RO membranes were prepared through IP between HPEA and TMC. As reactive monomers with multiple reaction sites, TMC and HPEA reacted with each other and formed the compact skin layer of RO membranes. In this preparation process, HPEA and TMC were dissolved in deionized water and hexane, respectively. The concentrations of HPEA and TMC were optimized with resultant concentrations of 2% (w/v) and 0.8% (w/v), respectively, to obtain membranes with good rejection and good permeation flux. Considering that DMAP, as a catalyst, could rapidly react with TMC to produce a light yellow precipitation, *N*-acylpyridinium salts, which has less solubility in the neutral starting materials than that in the polar solvents, DMAP was added into the aqueous phase instead of the organic phase. Due to the catalytic capacity, it is necessary to use only 0.05−0.2 mol of DMAP per mole of the secondary or tertiary alcohols.[42] A DMAP amount of 0.8 mol was used for per mole of HPEA because the HPEA molecule contains eight hydroxyl groups.

First, a polytetrafluoroethylene (PTFE) frame was fixed on the surface of the PSf-UF membrane. And the above-obtained HPEA aqueous solution was scattered on the PSf-UF membrane by directly pouring the solution into the frame. The excessive solution was drained off using a rubber roller after 20 min. The membrane surface was then scattered with TMC organic phase for another 20 min to carry out the IP between HPEA and TMC fully. A schematic illustration of the IP process is shown in Figure 1. Finally, the obtained composite membrane was heated at 60 °C for 20 min to attain the desired stability of the formed structure.

**2.3. Membrane Surface Characterization.** Scanning electron microscope (SEM, SIRION-100, FEI, Netherlands) was used to characterize the surface and cross-section morphologies of the blank PSf-UF membrane, PSf-HPEA composite membrane (no catalyst), and PSf-HPEA + DMAP composite membrane (catalyzed with DMAP). Attenuated total reflectance Fourier transform infrared spectroscopy (ATR-FTIR, Tensor 27, Bruker, Germany) was employed to obtain information about the chemical difference among these membranes. Other measurements, such as atomic force

Scheme 1. Schematic Diagram of the Membrane Performance Test Apparatus

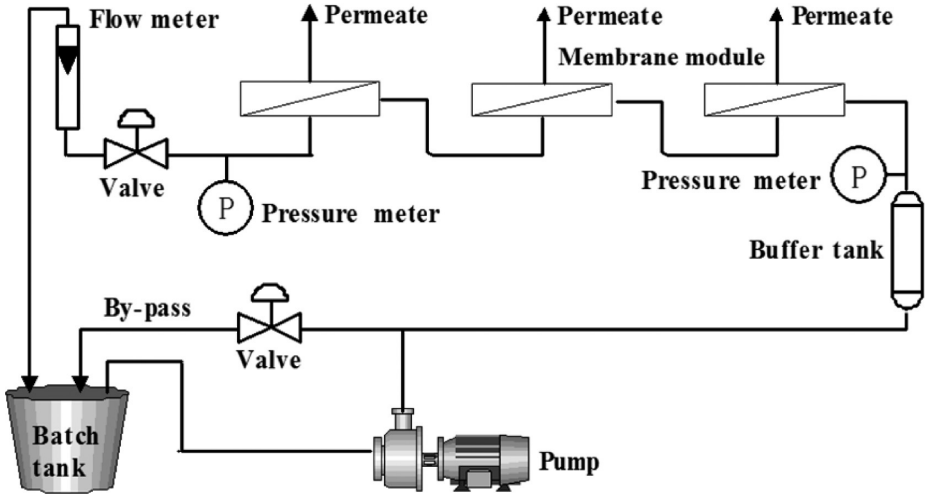


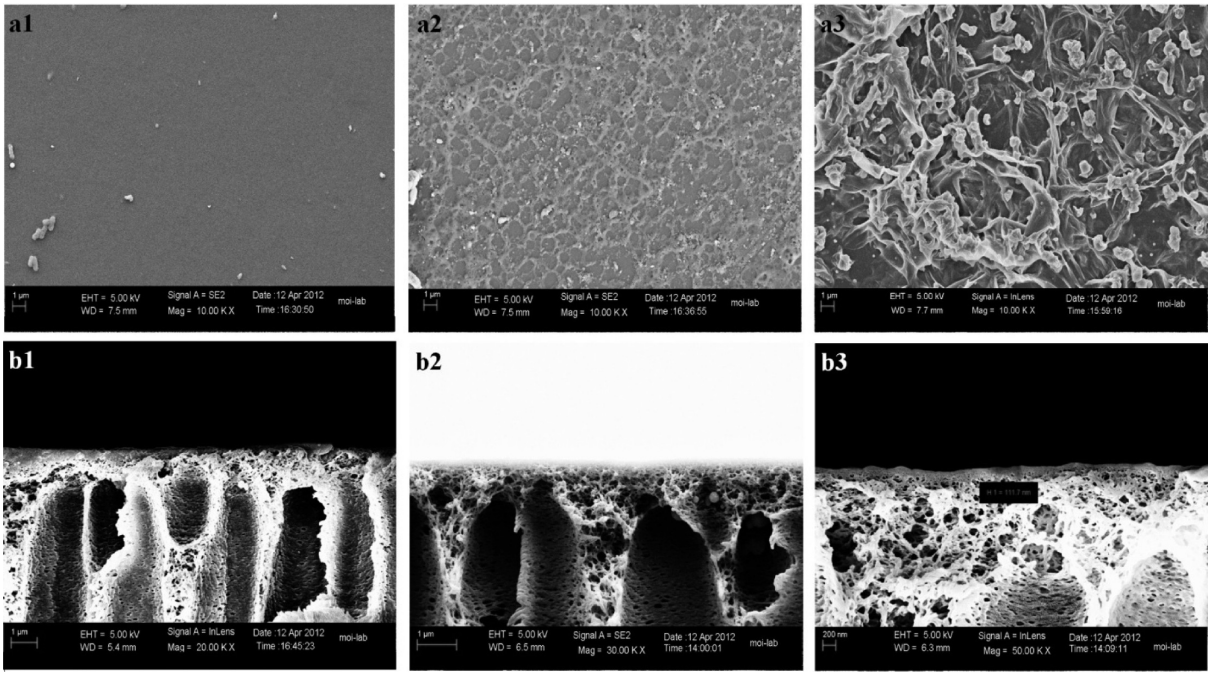


**Figure 2.** SEM images of membranes: (a) the surface microscope, (b) the cross-section microscope. (1) PSf-UF membrane, (2) PSf-HPEA composite membrane, and (3) PSf-HPEA + DMAP composite membrane.

microscopy (AFM, Agilent 5500, Agilent Technologies, France) and water contact angle (CA, Digidrop-DI, GBX, France) were also employed to characterize the composite membranes.

**2.4. Investigation of Membrane Separation Performance.** The composite membranes were set in the RO equipment (shown in Scheme 1) with a membrane area of 38.46 $cm^2$. The ultralow-pressure RO experiment was performed at the temperature of 25 °C and the pressure of 0.6 MPa. The separation performances of the composite membranes for NaCl, $Na_2SO_4$, and $MgSO_4$ aqueous solutions were tested by investigating their salt rejections (R) and water fluxes (F). And all concentrations of the salt solutions were 2000 mg $L^{-1}$. The accuracy concentrations of the feed and permeate were measured using a conductivity meter (model DDS-11A, Neici Instrument, Shanghai, China). The permeate and retentate were recycled back into the feed tank to keep the feed constant. A running time of 30 min at operating pressure was allowed before the rejection and flux tests. The separation performance for small electroneutral organic molecule, PEG-200 (1000 mg $L^{-1}$), of the composite membrane was also studied. LiquiTOC II (Elementar, Germany) was used to measure the concentration of the PEG-200 solution. The flux $F$ was obtained as follows:

$$F = \frac{V_P}{S\Delta t} \tag{1}$$

where $F$ ($L{\cdot}m^{-2}{\cdot}h^{-1}$) is the permeation flux of the composite membrane, $V_P$ (L) is volume of the permeate, $S$ ($m^2$) is the effective area of membrane, and $\Delta t$ (h) represents the operation time. And the rejection of the membrane was calculated by

$$R = \left(1 - \frac{C_P}{C_f}\right) \times 100\% \tag{2}$$

where $R$ (%) is the rejection of the membrane. $C_p$ and $C_f$ represent the permeate and feed concentration, respectively.

**2.5. Study of Membrane Physical–Chemical Stability.** Sometimes it is necessary for RO composite membrane to work in poor conditions. Therefore, the physical–chemical stabilities, including the chlorine-resistance ability, alkaline-resistance ability, and acid-

resistance ability of the as-prepared PSf-HPEA + DMAP composite membrane, were studied in our work. The physical−chemical stabilities were obtained by comparing the changes in the separation performances before and after the treatments. First, the separation performances of the PSf-HPEA + DMAP composite membranes were tested with 2000 mg $L^{-1}$ NaCl aqueous solution before the treatments. And the membranes were then immersed in HCl aqueous solution (0.5 mol $L^{-1}$) and NaOH aqueous solution (0.5 mol $L^{-1}$) for 12 h, respectively. After being rinsed, the separation performances of these membranes were tested again to investigate the acid-resistance and alkaline-resistance abilities. These treatments were repeated, and the permeability experiments were repeated six times. For chlorine-resistance ability, the membranes were immersed in NaClO aqueous solutions with free chlorine concentrations of 1000, 3000, 5000, 7000, and 9000 ppm for 1 h each. The membranes were rinsed with pure water before the tests of their water fluxes and salt rejections.

## 3. RESULTS AND DISCUSSION

**3.1. Surface Characteristics of Membranes.** SEM was employed to investigate the difference of the surface morphologies among the blank PSf-UF, PSf-HPEA composite membrane, and PSf-HPEA + DMAP composite membrane. Compared with the blank PSf-UF support membrane (Figure 2-a1), as shown in Figure 2-a2, largely discontinuous raised structures with obvious defects are formed on PSf support membrane when DMAP is absent, which indicates HPEA does not completely participate in the acylation. The SEM image of the PSf-HPEA + DMAP membrane (Figure 2-a3) exhibits a successive and rough film with a typical valley-clogging structure. Meanwhile, some nodules can be found on the active layer due to the aggregation of some HPEA and the intramolecule reaction of HPEA. These results agree with the existing studies.[6] The cross-section morphology (Figure 2-b3) of the PSf-HPEA + DMAP composite membrane clearly shows a thin layer with a thickness of about 110 nm, which is much thinner than that of conventional RO membranes with thicknesses of 200−500 nm.[6,7] In the case of PSf-HPEA composite membrane (Figure 2-b2), the obvious skin layer can hardly be observed. And a thinner skin layer with a more flawless structure will decrease the permeation resistance and endow the membrane with a much higher permeation flux and salt rejection. These results demonstrate that the catalytic effect of DMAP can significantly increase the membrane formation property of HPEA.

Figure 3 presents the ATR-FTIR spectra of HPEA-based composite membranes and blank PSf-UF supporting membrane. The results further prove the above-discussed SEM results. Compared with PSf-UF membrane, the absorption peak at 1805 $cm^{-1}$ (characteristic of the carbonyl of the ester bond) is found in the case of PSf-HPEA composite membrane, demonstrating the polymerization between HPEA and TMC, and the formation of a thin active layer on the PSf-UF membrane. At the same time, there are obvious absorption peaks at 1725 (C═O), 1250 (C−O), and 3423 $cm^{-1}$ ($\nu$O−H), indicating only part of the HPEA and TMC involved in the IP and the unreacted acyl chloride groups were hydrolyzed into carboxyl groups. Compared with PSf-HPEA composite membrane, the absorbance band at 3423 $cm^{-1}$ ($\nu$O−H) becomes much weaker in the case of the PSf-HPEA + DMAP membrane, existing only as a weak shoulder. While the absorbance signals at 1805 $cm^{-1}$, corresponding to the carbonyl (C═O) stretching frequency of the ester, is distinctly strengthened. This phenomenon indicates that it is the catalytic role of DMAP that makes more hydroxyl groups of HPEA react with the acyl groups of TMC to produce ester. On the other hand, numerous hydrophilic groups, including the unreacted hydroxyl and carboxyl groups, make it possible for the PSf-HPEA + DMAP composite membrane to own a high permeation flux.

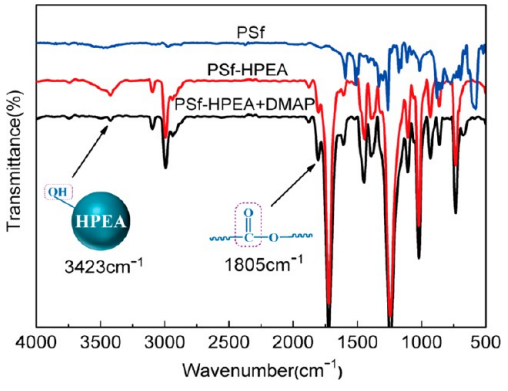


**Figure 3.** ATR-FTIR spectra of skin-layers of different membranes: PSf-UF membrane (blue), PSf-HPEA composite membrane (red), and PSf-HPEA + DMAP composite membrane (black).

Surface roughness of the RO membrane makes important influence on its permeability. As reported, a rougher membrane surface will promise a much higher permeation flux of RO membrane due to the much bigger superficial area.[44,45] The surface roughness of the PSf-HPEA + DMAP composite membrane was further studied by an AFM experiment (Figure 4). The resultant roughness of the PSf-HPEA + DMAP composite membrane is 102.2 nm, much higher than that of the traditional MPD/TMC RO membrane (with a roughness of about 42 nm).[46] And the AFM experimental result consists with the as-discussed observation of the SEM experiment result. This high roughness may result from the rigid molecular structure of both HPEA and TMC because of the existence of the benzene ring. The PSf-HPEA + DMAP composite membrane may easily form a concave−convex structure with such a rigid structure in the process of IP. In addition, the nodules on the membrane surface, produced by intramolecule reaction and aggregation of HPEA, increase the roughness of the PSf-HPEA + DMAP composite membrane.

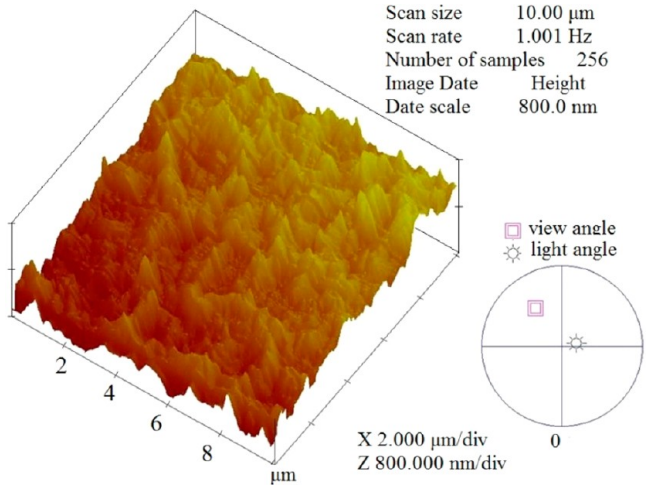


**Figure 4.** AFM image of the PSf-HPEA + DMAP composite membrane.

A water contact angle experiment was conducted to measure the hydrophilcity of the PSf-HPEA + DMAP composite membrane. The water contact angle of the prepared PSf-HPEA + DMAP composite membrane can reach 54°, showing strong hydrophilicity. This phenomenon may have two possible reasons. First, in the process of IP, for the organic phase, hexane volatilizes out and most of TMC are deposited on the surface of HPEA-based composite membrane. As a result, after the hydrolysis of acyl chloride groups, the membrane surface will be covered with a number of hydrophilic carboxyl groups.[47] And together with the influence of unreacted hydroxyl groups of HPEA molecules, due to the unique highly branched structure and the possession of many reactive terminal hydroxy groups of HPEA, the hydrophilicity of HPEA-based composite membranes will be surely improved. On the other hand, an increase in membrane surface roughness results in a decrease in the water contact angle when the water contact angle is smaller than 90°.[48] According to the result of AFM characterization, the PSf-HPEA + DMAP composite membrane owns high roughness and this makes contribution to the improvement of its hydrophility to some certain degree.

**3.2. Membrane Separation Performance.** The separation performances of the as-prepared composite membranes for the three different inorganic salt (NaCl, $Na_2SO_4$, and $MgSO_4$) solutions were investigated and compared as shown in Figure 5.

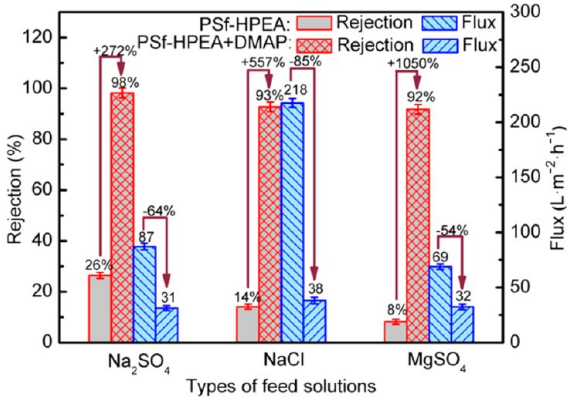


**Figure 5.** Permeation performance of HPEA-based composite membranes for different salts at $P$ = 0.6 MPa and $T$ = 25 °C.

By comparing the corresponding data, it can be inferred that PSf-HPEA + DMAP membrane exhibits very good permeation property of ultralow-pressure RO membrane. The rejections for all types of salts in the case of PSf-HPEA + DMAP membrane increase dramatically by more than 70% compared with those of the PSf-HPEA composite membrane. Especially for $Na_2SO_4$ solution, the salt rejection is up to 98.2% simultaneously with a relatively high flux of 31 L·m$^{-2}$·h$^{-1}$ even at the operating pressure of 0.6 MPa. The rejections of $Na_2SO_4$ and NaCl are higher than that of $MgSO_4$, which could be attributed to the negative charge on the PSf-HPEA + DMAP membrane surface because of the carboxyl groups caused by TMC hydrolysis. Due to the much better developed three-dimensional structure than traditional PA RO membrane and intramolecules nanovoids of cross-linked HPEA layer, the resulting membranes also exhibit a very high water permeation flux even at an ultralow pressure (0.6 MPa). The significant improvement of the separation performance results from the unique three-dimensional network structure, the numerous hydrophilic surface groups, and the catalysis of DMAP. In which, the rigid molecule structures (Supporting Information Figure S2) of HPEA and TMC can decrease the rotation and vibration of molecular chains and thus endow the active layer with excellent rejection for different salts solutions even with a thickness of only about 100 nm. The rough surface as well as the adequate hydrophilic hydroxyl and carboxyl groups is the guarantee of permeation flux. What's more, HPEA can also cross-link with TMC and form a kind of well-developed three-dimensional network structure because of the molecular structural characteristic of the HPEA. Different with the one-dimensional network structure, formed by the cross-linking between TMC and *m*-phenylenediamine (MPD), this structure can eliminate the trade-off trend between water flux and salt rejection. For these reasons, the as-prepared PSf-HPEA + DMAP composite membrane owns both very high water flux and satisfactory salt rejection.

As mentioned above, the charge of the as-prepared membranes surfaces will affect the rejections of different salts to a certain degree. Therefore, the permeation performances of the as-prepared membranes for the electrically neutral PEG-200 were investigated to avoid the influence of the membrane surface charge and further explore the evidence of the catalysis of DMAP to the cross-linking reaction between HPEA and TMC (Figure 6). The rejections for PEG-200 of the HPEA-

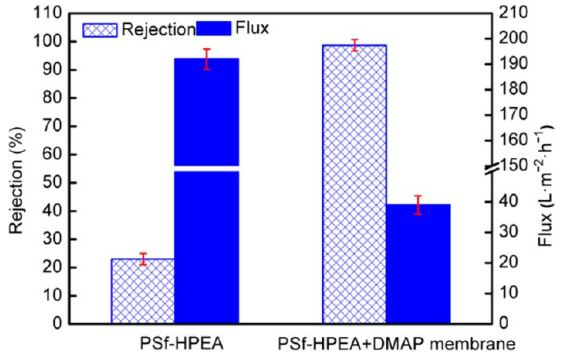


**Figure 6.** Permeation performance of the HPEA-based composite membranes for PEG-200 at $P$ = 0.6 MPa and $T$ = 25 °C.

based composite membranes greatly increase from 23% to 98% after the addition of DMAP. The flux of the PSf-HPEA + DMAP membrane can reach nearly 40 L·m$^{-2}$·h$^{-1}$ at the same time even with an operation pressure of 0.6 MPa. And the potential of PSf-HPEA+DMAP composite membrane showing in our study provides a promising strategy for removing small organic molecules from water.

**3.3. Catalytic Mechanism of DMAP.** The studies of Hassner[49] revealed that the nitrogen atom located on the pyridine cycle and the dimethylamino groups outside the ring that enables DMAP to have high catalytic activity toward the phase transfer reaction and acylation. Combined with the catalytic cycle of DMAP proposed by Spivey and co-workers,[50] we tried to describe the catalytic effect of DMAP on this hyperbranched polymers based on IP. The detailed catalytic process can be divided into two cycles (see the Supporting Information for more details).

In the first cycle, DMAP could function as the phase transfer catalyst (PTC). This kind of PTC can be defined as the R4NX type because of the two tertiary amino groups inside and outside of the pyridine ring (Supporting Information Figure S1a). When added into the aqueous phase, DMAP was first formed into an ion pair with HPEA. The ion pair was then


dx.doi.org/10.1021/am401345y | ACS Appl. Mater. Interfaces 2013, 5, 6649−6656

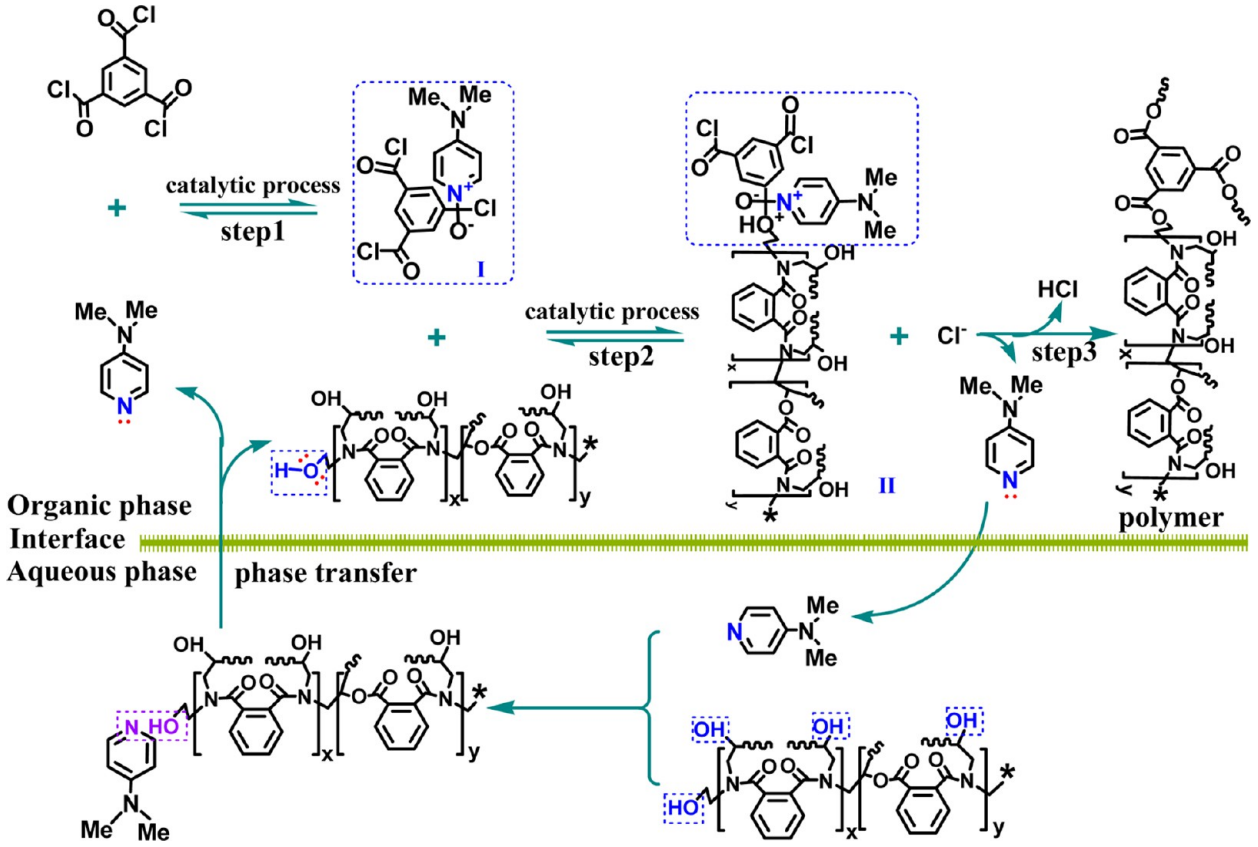


**Figure 7.** Catalytic mechanism of DMAP catalyzing interfacial polymerization based on HPEA.

rapidly extracted into the organic phase to reduce the steric hindrance of HPEA during the diffusion in the organic phase and to increase the probability of the collision of molecules. The detailed process is shown in Supporting Information Figure S3.

In the second cycle, DMAP was served as an efficacious nucleophilic acylation catalyst. When substituted with the electron-donating 2-alkyl groups, the pyridine ring of DMAP strongly resonated with the exocyclic nitrogen atom and thus obtained a high density of electron cloud, which drastically enhanced the nucleophilic ability of the nitrogen atom over the ring. Therefore, facilitating the formation of steady intermediate acylpyridinium salts from the catalyst and TMC was easy. Compared with TMC, such intermediate salts with "loose" delocalized ion pairs were more easily attacked by the electrophilic reagent under the acid/base catalysis. This cycle is similar to Steglich esterification as shown in Figure 7. Reversible formation of *N*-acylpyridinium salt I through the attack of DMAP dissociated from the former phase transfer to the acyl donor TMC (step 1) is followed by reversible nucleophilic addition of HPEA to salt I (step 2) with a concomitant proton transfer promoted by the anions $Cl^-$ (through transition step 3) and finally elimination to regenerate the catalyst (Supporting Information Figure S4).

**3.4. Physical–Chemical Stability.** Chlorine-resistance ability is an important index for the physical–chemical stability of the RO composite membrane. The RO composite membrane must work in particular conditions that contain active chlorine at a specific concentration in most cases. However, traditional polyamide (PA) RO membranes usually have poor resistance to chlorine. That is because under the attack of free chlorine, the formation of *N*-halamine and the Orton rearrangement are easy to happen, resulting in the break of amido bonds.[51−53] The experiment result, shown in Figure 8,

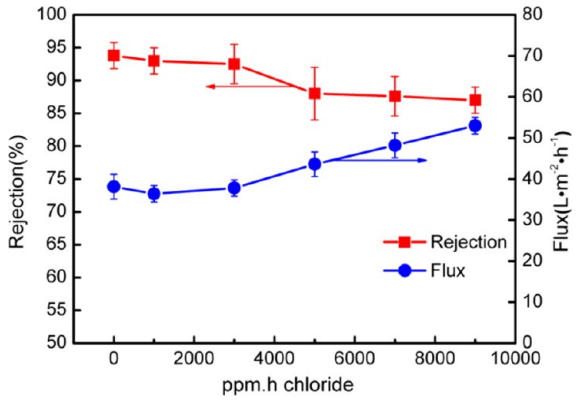


**Figure 8.** Performance of the PSf-HPEA + DMAP composite membrane before and after treatment with the NaClO aqueous solution (measured with a 2000 mg $L^{-1}$ NaCl aqueous solution at 25 °C and 0.6 MPa).

indicates the PSf-HPEA + DMAP composite membrane owns good chlorine-resistance ability. Rejection slightly decreases to about 90% even after exposing the membrane to 4000 ppm h of free chlorine. And in the entire process of the experiment, the rejection of the membrane only decreases from 93% to 87%, and the water flux increases from 38 to 53 $L{\cdot}m^{-2}{\cdot}h^{-1}$.

It is obvious to find that the acid-resistance ability of this membrane is poor (according to Figure 9). The rejection of NaCl obviously decreases after the acid treatment possibly because HPEA and TMC cross-link with each other through an


dx.doi.org/10.1021/am401345y | ACS Appl. Mater. Interfaces 2013, 5, 6649−6656

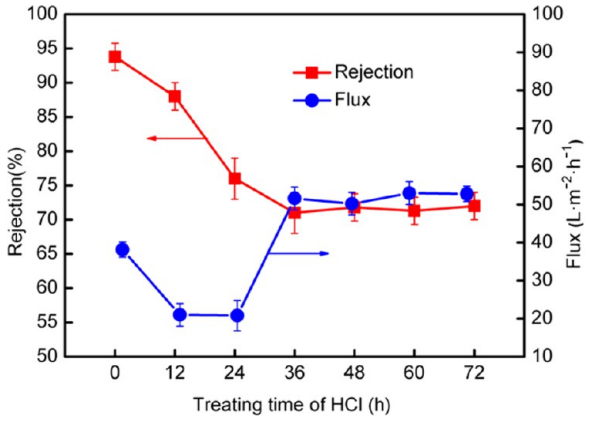


**Figure 9.** Performance of the PSf-HPEA + DMAP composite membrane before and after treatment with the 0.5 mol $L^{-1}$ HCl aqueous solution (measured with a 2000 mg $L^{-1}$ NaCl aqueous solution at 25 °C and 0.6 MPa).

ester bond, which can be easily hydrolyzed in an acid solution. The water flux of the composite membrane initially decreases and then increases. This phenomenon may be attributed to the damaged molecular chains that block the spaces in the three-dimensional network structure during the initial stage of the acid treatment. While the further treatment could clear the blockages and recover the normal water flux of the composite membrane. With the treatment for 36 h, the rejection and water flux of the composite membrane is trending toward stability of about 71% and 52 $L{\cdot}m^{-2}{\cdot}h^{-1}$, respectively.

In addition, the alkaline-resistance ability of the PSf-HPEA + DMAP composite membrane, exhibiting in the experiment, is much poorer even than the acid-resistance ability. The rejection of the composite membrane decreases by nearly 50% when treated with the NaOH solution as shown in Figure 10. At the

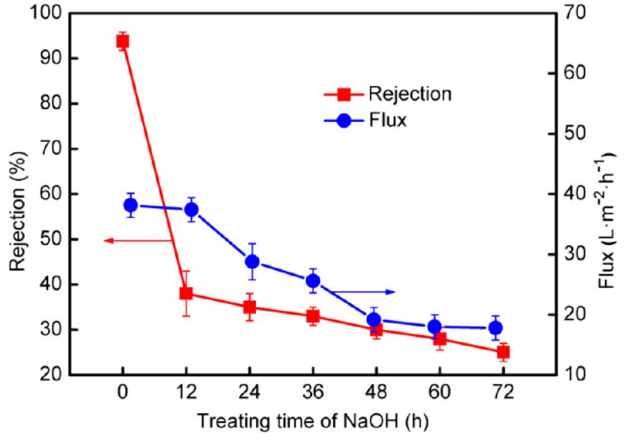


**Figure 10.** Performance of the PSf-HPEA + DMAP composite membrane before and after the treatment with the 0.5 mol $L^{-1}$ NaOH aqueous solution (measured with a 2000 mg $L^{-1}$ NaCl aqueous solution at 25 °C and 0.6 MPa).

same time, it is interesting to find that the water flux decreases during the entire process of the alkaline treatment. This result demonstrates that the surface structure of the PSf-HPEA + DMAP composite membrane is seriously damaged and that the spaces are blocked by the damaged molecular chains when treated with the NaOH solution.

## 4. CONCLUSION

In summary, we provided a feasible way to prepare RO membranes based on hyperbranched polymers with DMAP as the multifunctional catalyst. The addition of DMAP into the aqueous phase significantly increased the degree of the cross-link reaction between highly steric-hindered HBPs and TMC. A dense composite membrane that possessed good permeation properties was obtained. This membrane shows the possibility of preparing a high-performance composite membrane through interfacial chain propagation polymerization based on branched macromolecules. The catalytic mechanism of DMAP shows that the catalytic effect can be further improved by increasing the electron density of the substitution groups. More detailed conclusions need further research, and related work is under investigation. The excellent separation performances for the PEG-200 solution as well as salt solutions even at ultralow-pressure and good chlorine-resistance ability show the promising application of the PSf-HPEA + DMAP composite RO membrane in water treatment.

## ■ ASSOCIATED CONTENT

### Ⓢ Supporting Information

Two cycles of the catalytic mechanism of DMAP in interfacial polymerization between HPEA and TMC. This material is available free of charge via the Internet at http://pubs.acs.org.

## ■ AUTHOR INFORMATION

### Corresponding Author

*E-mail: linzhang@zju.edu.cn. Tel. and Fax: +86-571-87952121.

### Notes

The authors declare no competing financial interest.

## ■ ACKNOWLEDGMENTS

This work was supported by National Natural Science Foundation of China (21076176); the National Basic Research Program of China (2009CB623402); and Natural Science Foundation of Zhejiang Province (LR12B06001).

## ■ REFERENCES

(1) Menachem, E.; Phillip, W. A. *Science* **2011**, *333*, 712−717.
(2) Shannon, M. A.; Bohn, P. W.; Elimelech, M.; Georgiadis, J. G.; Mariñas, B. J.; Mayes, A. M. *Nature* **2008**, *452*, 301−310.
(3) Petersen, R. J. *J. Membr. Sci.* **1993**, *83*, 81−150.
(4) Gelse, G. M.; Lee, H. S.; Miller, D. L.; Freeman, B. D.; Mcgrath, J. E.; Paul, D. R. *J. Polym. Sci., Part B: Polym. Phys.* **2010**, *48*, 1685−1718.
(5) Zou, H.; Jin, Y.; Yang, J.; Dai, H. G.; Yu, X. L.; Xu, J. *Sep. Purif. Technol.* **2010**, *72*, 256−262.
(6) Qiu, S.; Wu, L. G.; Zhang, L.; Chen, H. L.; Gao, C. J. *J. Appl. Polym. Sci.* **2009**, *112*, 2066−2072.
(7) Ahmad, A. L.; Ooi, B. S. *J. Membr. Sci.* **2005**, *255*, 67−77.
(8) Lind, M. L.; Ghosh, A. K.; Jawor, A.; Huang, X.; Hou, W.; Yang, Y.; Hoek, E. M. V. *Langmuir* **2009**, *25*, 10139−10145.
(9) Choi, O.; Deng, K. K.; Kim, N.-J.; Ross, L., Jr.; Surampalli, R. Y.; Hu, Z. *Water Res.* **2008**, *42*, 3066−3074.
(10) Jeong, B.-H.; Hoek, E. M. V.; Yan, Y.; Subramani, A.; Huang, X.; Hurwitz, G.; Ghosh, A. K.; Jawor, A. *J. Membr. Sci.* **2007**, *294*, 1−7.
(11) Lee, S. Y.; Kim, H. J.; Patel, R.; Im, S. J.; Kim, J. H.; Min, B. R. *Polym. Adv. Technol.* **2007**, *18*, 562−568.
(12) Huang, H.; Qu, X. Y.; Dong, H.; Zhang, L.; Chen, H. L. *RSC Adv.* **2013**, *3*, 8203−8207.
(13) Lind, M. L.; Suk, D. E.; Nguyen, T.-V.; Hoek, E. M. V. *Environ. Sci. Technol.* **2010**, *44*, 8230−8235.

(14) Tiraferri, A.; Kang, Y.; Giannelis, E. P.; Elimelech, M. *ACS Appl. Mater. Interfaces* **2012**, *4*, 5044−5053.
(15) Fathizadeh, M.; Aroujalian, A.; Raisi, A. *J. Membr. Sci.* **2011**, *375*, 88−95.
(16) Kim, C. K.; Kim, J. H.; Roh, I. J.; Kim, J. J. *J. Membr. Sci.* **2000**, *165*, 189−199.
(17) Chen, G.; Li, S.; Zhang, X.; Zhang, S. *J. Membr. Sci.* **2008**, *310*, 102−109.
(18) Xu, J.; Feng, X.; Gao, C. *J. Membr. Sci.* **2011**, *370*, 116−123.
(19) Wei, X.; Wang, Z.; Zhang, Z.; Wang, J.; Wang, S. *J. Membr. Sci.* **2010**, *351*, 222−233.
(20) Sarkar, A.; Carver, P. I.; Zhang, T.; Merrington, A.; Bruza, K. J.; Rousseau, J. L.; Keinath, S. E.; Dvornic, P. R. *J. Membr. Sci.* **2010**, *349*, 421−428.
(21) Wei, X.; Wang, Z.; Chen, J.; Wang, J.; Wang, S. *J. Membr. Sci.* **2010**, *346*, 152−162.
(22) Wu, D.; Liu, X.; Yu, S.; Liu, M.; Gao, C. *J. Membr. Sci.* **2010**, *352*, 76−85.
(23) Arena, J. T.; McCloskey, B.; Freeman, B. D.; McCutcheon, J. R. *J. Membr. Sci.* **2011**, *375*, 55−62.
(24) Yu, S.; Lue, Z.; Chen, Z.; Liu, X.; Liu, M.; Gao, C. *J. Membr. Sci.* **2011**, *371*, 293−306.
(25) Seiler, M. *Fluid Phase Equilib.* **2006**, *241*, 155−174.
(26) Gao, C.; Yan, D. *Prog. Polym. Sci.* **2004**, *29*, 183−275.
(27) Kim, Y. H. *J. Am. Chem. Soc.* **1992**, *114*, 4947−4948.
(28) Fogelström, L.; Malmström, E.; Johansson, M.; Hult, A. *ACS Appl. Mater. Interfaces* **2010**, *2*, 1679−1684.
(29) Maji, P. K.; Guchhait, P. K.; Bhowmick, A. K. *ACS Appl. Mater. Interfaces* **2009**, *1*, 289−300.
(30) Wu, C.; Huang, X. Y.; Wang, G. L.; Wu, X. F.; Yang, K.; Li, S. T.; Jiang, P. K. *J. Mater. Chem.* **2012**, *22*, 7010−7019.
(31) Zhao, Y. H.; Zhu, B. K.; Ma, X. T.; Xu, Y. Y. *J. Membr. Sci.* **2007**, *290*, 222−229.
(32) Chung, T. S.; Chng, M. L.; Pramoda, K. P.; Xiao, Y. C. *Langmuir* **2004**, *20*, 2966−2969.
(33) Sun, S. P.; Hatton, T. A.; Chung, T. S. *Environ. Sci. Technol.* **2011**, *45*, 4003−4009.
(34) Sim, Y. H.; Wang, H.; Li, F. Y.; Chua, M. L.; Chung, T. S.; Toriida, M.; Tamai, S. *Carbon* **2013**, *53*, 101−111.
(35) Suzuki, T.; Yamada, Y. *J. Appl. Polym. Sci.* **2013**, *127*, 316−322.
(36) Li, L. C.; Wang, B. G.; Tan, H. M.; Chen, T. L.; Xu, J. P. *J. Membr. Sci.* **2006**, *269*, 84−93.
(37) Chiang, Y. C.; Hsub, Y. Z.; Ruaan, R. C.; Chuang, C. J.; Tun, K. L. *J. Membr. Sci.* **2009**, *326*, 19−26.
(38) Wei, X. Z.; Zhu, L. P.; Deng, H. Y.; Xu, Y. Y.; Zhu, B. K.; Huang, Z. M. *J. Membr. Sci.* **2008**, *323*, 278−287.
(39) Zhang, L.; Lin, S. S.; Wei, P.; Cheng, L. H.; Chen, H. L. *Chin. J. Catal.* **2012**, *33*, 1730−1735.
(40) Höfle, G.; Steglich, W. *Synthesis* **1972**, *11*, 619−621.
(41) Ragnarsson, U.; Grehn, L. *Acc. Chem. Res.* **1998**, *31*, 494−501.
(42) Höfle, G.; Steglich, W.; Vorbrueggen, H. *Angew. Chem., Int. Ed. Engl.* **1978**, *17*, 569−583.
(43) Mathias, L. J.; Vaidyat, R. A. *J. Am. Chem. Soc.* **1986**, *108*, 1093−1094.
(44) Freger, V. *Langmuir* **2003**, *19*, 4791−4797.
(45) Hirose, M.; Ito, H.; Kamiyama, Y. *J. Membr. Sci.* **1996**, *121*, 209−215.
(46) Kwak, S. Y.; Jung, S. G.; Yoon, Y. S.; Ihm, D. W. *J. Polym. Sci., Part B: Polym. Phys.* **1999**, *37*, 1429−1440.
(47) Ghosh, A. K.; Jeong, B.-H.; Huang, X.; Hoek, E. M. V. *J. Membr. Sci.* **2008**, *311*, 34−45.
(48) Wenzel, R. N. *Ind. Eng. Chem. Res.* **1936**, *28*, 988−994.
(49) Hassner, A.; Krepski, L. R.; Alexanian, V. *Tetrahedron* **1978**, *34*, 2069−2076.
(50) Spivey, A. C.; Arseniyadis, S. *Angew. Chem., Int. Ed.* **2004**, *43*, 5436−5441.
(51) Buch, P. R.; Mohan, D. J.; Reddy, A. V. R. *J. Membr. Sci.* **2008**, *309*, 36−44.
(52) Kawaguchi, T.; Tamura, H. *J. Appl. Polym. Sci.* **1984**, *29*, 3359−3367.
(53) Antony, A.; Fudianto, R.; Cox, S.; Leslie, G. *J. Membr. Sci.* **2010**, *347*, 159−164.